Epitaxial explosive crystallization of amorphous silicon

A. Polman, D. J. W. Mous, P. A. Stolk, and W. C. Sinke
FOM-Institute for Atomic and Molecular Physics, Kruislaan 407, 1098 SJ Amsterdam, The Netherlands

C. W. T. Bulle-Lieuwma and D. E. W. Vandenhoudt
Philips Research Laboratories, P. O. Box 80 000, 5600 JA Eindhoven, The Netherlands

(Received 6 April 1989; accepted for publication 6 July 1989)

It is shown that amorphous silicon can be transformed to monocrystalline silicon via an explosive epitaxial crystallization process induced by pulsed laser irradiation. 370-nm-thick amorphous Si layers, buried beneath a 130-nm-thick crystalline surface layer, were irradiated with a 32 ns ruby laser pulse. Real-time reflectivity measurements indicate that internal melting can be initiated at the amorphous-crystalline interface, immediately followed by explosive crystallization of the buried amorphous Si layer. Channeling and cross-sectional transmission electron microscopy reveal that explosive crystallization proceeds epitaxially with formation of twins extending into the sample. The crystal growth velocity is determined to be 16.2 ± 1.2 m/s, close to the fundamental limit for crystalline ordering at a liquid Si/Si(100) interface.

The amorphous phase of silicon (*a*-Si) is metastable with respect to the crystalline phase (*c*-Si).[1] Under moderate heating conditions, *a*-Si transforms directly into *c*-Si. Under rapid heating conditions, however, *a*-Si, if heated above its melting temperature, transforms to the metallic liquid state (*l*-Si).[2] Upon cooling, this phase solidifies to either the amorphous or the crystalline phase, depending on the quench rate[3] and the presence of a seed for crystallization.[4,5] Despite the important role of silicon in present day semiconductor technology, the fundamental mechanisms behind these phase transformations are still poorly understood.

Important insight into the thermodynamics and kinetics of these transformations can be obtained from a study of "explosive" crystallization of the amorphous phase. This process has been shown to occur in ion-implanted amorphized Si surface layers following nanosecond pulsed laser irradiation.[2,6-12] Under specific conditions of irradiation and sample structure, a shallow region of *a*-Si at the surface is heated and melted, whereupon a self-propagating ("explosive") melting and solidification process, driven by the difference in latent heat of *a*-Si and *c*-Si, transforms the *a*-Si layer to *c*-Si. Explosive crystallization (EC) of amorphous surface layers yields randomly oriented, fine-grain ($\approx$100 Å) polycrystalline Si.[2,7,8,10] This microstucture originates from the specific *c*-Si nucleation events which sustain EC. The precise nature of the processes that trigger and sustain EC is still under debate.[10,13,14]

In this letter a new type of explosive crystallization is presented, induced in a *c*-Si(100) sample which contains an *a*-Si layer buried beneath the surface. It is found that, using a pulsed laser, melting can be initiated buried in the sample at the *c*-Si/*a*-Si interface, whereupon *epitaxial explosive crystallization* is initiated from the crystalline "seed" at the surface.

Single crystals of Si with (100) oriented polished surfaces were implanted at room temperature with 450 keV $^{63}Cu^+$ ions to a total dose of 1.5×10^{15} cm^{-2} using a (011) planar channeling geometry. The sample was tilted 7° from a plane perpendicular to the ion beam, with the tilt axis parallel to a [011] wafer flat. The ion beam was scanned electrostatically, with an angular divergence of 1°. Using these channeling conditions, a sample containing a buried amorphous layer was produced, as will be shown later. Following implantation, samples were irradiated with a *Q*-switched ruby laser ($\lambda = 694$ nm, pulse duration 32 ns full width at half maximum). To study the phase transformations during irradiation in real time, transient optical reflectivity measurements[15] were employed using a 15 mW continuous-wave AlGaAs laser operating at $\lambda = 825$ nm. After irradiation, 2.0 MeV He^+ Rutherford backscattering spectrometry (RBS) and cross-sectional transmission electron microscopy (TEM) were performed to study the sample microstructure.

Figure 1 shows a comparison of RBS spectra for a sample after implantation analyzed in a channeling and a random direction. The channeling spectrum shows a reduced yield near the Si surface backscattering energy, indicating that a surface layer has remained crystalline with a low defect concentration (region I in the figure). The thickness of this layer is calculated to be approximately 130 nm. The high-yield portion (regions II and III) in this spectrum corresponds to a buried disordered layer with a thickness of

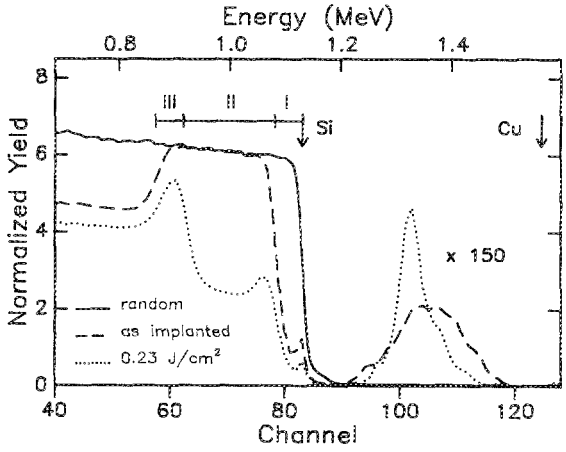

FIG. 1. Channeling RBS spectra for Si (100) samples implanted in a planar channeling geometry with 450 keV ^{63}Cu ions to a total dose of 1.5×10^{15} cm^{-2}. Spectra before and after irradiation at 0.23 J/cm^2 are shown. Channeling was performed with the ion beam aligned with the [100] axis. A random spectrum is shown for reference. Surface backscattering energies for Si and Cu are indicated by arrows.

 0003-6951/89/371097-03$01.00

$\approx$485 nm. This region includes both an amorphous layer and a deeper lying region containing implantation tail damage which is usually observed in ion implantation.

Figure 2 shows a compilation of time-resolved reflectivity measurements performed during pulsed laser irradiation at several energy densities. Below 0.13 J/cm^2, no change in the reflectivity is detected. For 0.20 and 0.23 J/cm^2 pronounced oscillations are observed. As has been shown earlier,[8-11] such behavior is strongly indicative of a planar solid-liquid interface moving into the interior of the sample; the measured intensity results from interference of light reflected from the sample surface and from a moving buried interface. The following melting and solidification scenario is suggested for low-energy irradiation. During the laser pulse, melting is initiated in the buried a-Si layer due to the lower melting temperature of a-Si ($T_{ma} \approx 1460$ K[12]) relative to that of c-Si ($T_{mc} = 1685$ K) and as a result of the higher absorption coefficient of a-Si. This heavily undercooled (temperature $\approx T_{ma} < T_{mc}$) liquid layer crystallizes immediately at the interface with the c-Si surface layer. The heat released upon solidification is used to melt deeper lying a-Si. This deeper, undercooled liquid layer will crystallize, again releasing latent heat, and hence a self-sustaining ("explosive") melting and crystallization process occurs in the buried a-Si layer.

Optical calculations[16] show that the reflectivity will decrease with respect to the initial value as soon as a buried liquid layer forms at 130 nm depth. This is a result of destructive interference between light reflected from the surface and from the buried c-Si/l-Si interface and is clearly observed in the reflectivity transients in Fig. 2. Following this initial decrease, subsequent interference maxima and minima are expected for every 52 nm (= 1/4 wavelength in the sample) the buried liquid layer propagates into the sample. These interference effects are clearly observed for 0.20 and 0.23 J/cm^2. For 0.20 J/cm^2 irradiation, the buried layer moves from the original c-Si/a-Si interface at 130 nm to a depth of $\approx$500 nm from the surface. From the timing of the extrema the EC velocity is calculated: 16.2 $\pm$ 1.2 m/s, constant over the depth within the error.[16] Interference extrema are also observed for other energy densities between 0.13 and 0.20 J/cm^2; however, they are less in number, indicating that the EC process was quenched in the a-Si layer.

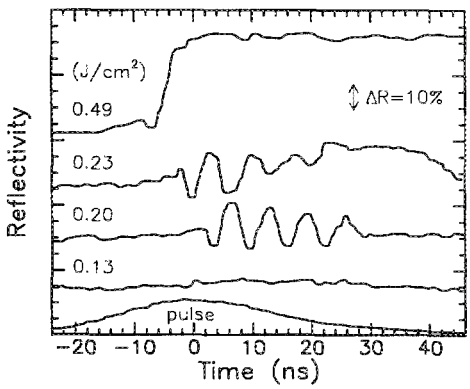

FIG. 2. Transient reflectivity measurements recorded during pulsed laser irradiation at different laser energy densities (indicated in the figure). The laser pulse profile is shown at the bottom. Reflectivity transients are shifted for clarity and the arrow indicates the reflectivity scale.

At 0.23 J/cm^2 an increase in reflectivity superimposed on the last few extrema is observed. For higher energy densities this effect becomes more pronounced; in the reflectivity transient for 0.49 J/cm^2, a high-reflectivity plateau is observed after the initial decrease in reflectivity. The absolute value of this plateau ($R = 75\%$) corresponds to that of an optically thick liquid layer at the sample surface. This layer shields the buried l-Si layer from the probe laser light and hence no further oscillations in reflectivity are observed. This indicates that at high-energy irradiation, after initiation of melting in the buried a-Si layer, the laser pulse still supplies sufficient energy to raise the surface temperature above the melting point (T_{mc}).

A channeling spectrum for the sample irradiated at 0.23 J/cm^2 is shown in Fig. 1. A drastic decrease is observed in the yield from the originally amorphous layer (region II indicated in the figure). This implies that the amorphous layer has crystallized with a large degree of order in the [100] direction. In addition, Fig. 1 shows a magnification of the Cu backscattering signal before and after irradiation. After irradiation, the Cu profile has shifted to lower backscattering energies, indicating that Cu has been transported inward into the sample. This is further evidence that a buried liquid layer has moved through the sample: Cu exhibits strong segregation effects at the l-Si/c-Si interface and thus is zone-refined inward, with the self-propagating liquid layer.[6]

Both the reduction in channeling yield and the Cu segregation have been studied for an extended range of irradiation energy densities[17] and show the same effect at all energy densities between 0.2 and 0.5 J/cm^2. Cross-sectional TEM was employed on a sample irradiated at an intermediate energy density of 0.35 J/cm^2. In the TEM micrograph [Fig. 3(a)], three distinct regions can be observed on top of the c-Si substrate.

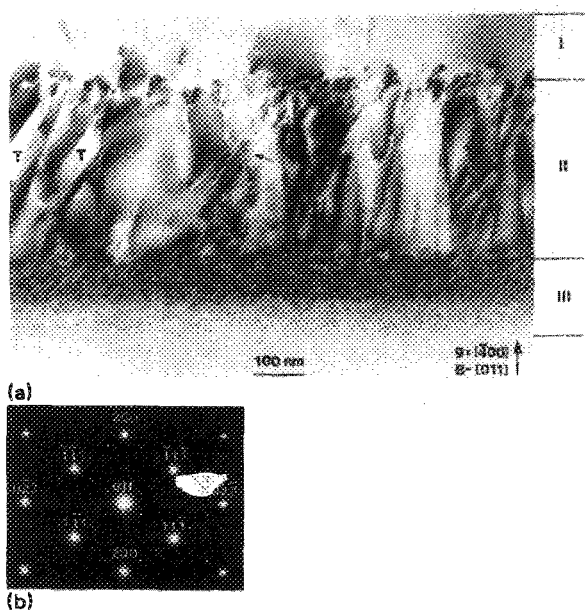

FIG. 3. (011) cross-sectional TEM micrograph. (a) [$\bar{4}$00] bright field image after pulsed laser irradiation at 0.35 J/cm^2. (b) Electron diffraction pattern from the crystallized Si layer. Images of primary spots mirrored with respect to the axis through [$\bar{1}$11] and [11$\bar{1}$] or with respect to the axis through [1$\bar{1}$1] and [$\bar{1}$1$\bar{1}$] correspond to twinned regions. Other spots are attributed to double diffraction.

(I) A 130-nm-thick crystalline surface layer. The top 100 nm of this layer contains a low density of dislocations and microtwins. High-resolution microscopy shows that a large density of small (≈ 100 Å) microtwins has formed in the interface area with region II. Twins are oriented parallel to {111} planes, inclined at 35° to the surface normal. The total thickness of region I corresponds to that of the *c*-Si surface layer of the as-implanted sample as inferred from the channeling spectrum in Fig. 1.

(II) The originally amorphous region, which was explosively crystallized (thickness 370 nm). Selected-area electron diffraction [Fig. 3(b)] reveals that this region is monocrystalline with the same orientation as the surface region. However, besides the bright spots of the Si matrix, small spots corresponding to twins are observed. Such twinned regions can be identified in the bright field image of Fig. 3(a) and are marked *T*. In this micrograph also, boundaries parallel to [100] can be seen (marked by arrows). This strongly suggests that epitaxial crystallization proceeds via growth of [100] columns. The lateral dimension of these columns is 50–200 nm. Using high-resolution microscopy, a large density of microtwins is observed along these boundaries. The longer twin lamellae extending deep into the crystallized layer originate from these boundaries. No amorphous or randomly oriented polycrystalline areas are detected in region II. The 40% backscattering yield as observed in channeling from this region (see Fig. 1) is attributed to direct scattering from twinned regions or slightly misaligned columns as well as to dechanneling from microtwins at the interface between I and II.

(III) A defected region (thickness ≈ 160 nm) beneath the crystallized layer. The dark contrast in the micrograph is characteristic of implantation-tail damage. The darkest, most heavily damaged part of this region corresponds to the high-yield portion (region III) in the channeling spectrum of the irradiated sample in Fig. 1.

This study shows that amorphous layers buried in a crystalline matrix can be crystallized epitaxially using pulsed laser irradiation. Melting is initiated at the *c*-Si/*a*-Si interface, whereupon epitaxial explosive crystallization is immediately initiated at the monocrystalline surface seed. Nonplanarity of the interface from which EC is seeded, or transient stress effects related to the difference in density between solid and liquid Si, may lead to the nonperfect epitaxy, with columnar growth and twin formation. Additional experiments, using ^{31}P, ^{40}Ar, ^{115}In ion implantation, as well as using ^{28}Si self-implantation, show qualitatively the same behavior in a whole range of sample structures.[17] Transient conductivity measurements[17] on samples with a different buried *a*-Si layer thickness, combined with calculations, suggest that in the present experiments the buried liquid layer reaches a maximum thickness of ≈ 40 nm.

No microcrystalline grains were observed after EC, which indicates that the nucleation and growth processes which sustain explosive crystallization of amorphous surface layers and which yield randomly oriented polycrystalline Si, do not occur under the present experimental conditions. Such processes may involve heterogeneous nucleation at the leading *a*-Si/*l*-Si interface, as suggested by Tsao and Peercy,[13] or solid-state nucleation in *a*-Si during the heating period prior to melting, as suggested by Roorda and Sinke.[14] Alternatively, in the present experiments the buried layer crystallizes via solidification at the trailing interface with *c*-Si. The average EC velocity in the Cu-implanted samples is 16.2 ± 1.2 m/s, constant over the depth. Additional experiments using Si-implanted samples[17,18] show that the Cu impurity does not influence the EC velocity to a measurable extent. Similar velocities for epitaxial crystal growth have also been observed in other experiments, e.g., by Thompson *et al.*[3] and Cullis *et al.*[19] The present data, however, are the first to show self-sustained crystallization at this high rate. The velocity is close to the maximum speed for crystalline ordering at a *l*-Si/*c*-Si (100) interface (i.e., 15 ± 1.5 m/s for intrinsic Si), above which amorphous phase formation has been observed to occur.[3]

The authors would like to thank A. G. Cullis (RSRE, Malvern) for helpful discussions. The work at the FOM-Institute is part of the research program of FOM and was made possible by financial support from Stiching voor Technische Wetenschappen and Nederlandse organisatie voor Wetenschappelijk Onderzoek.

[1] E. P. Donovan, F. Spaepen, D. Turnbull, J. M. Poate, and D. C. Jacobson, Appl. Phys. Lett. **42**, 698 (1983).
[2] M. O. Thompson, G. J. Galvin, J. W. Mayer, P. S. Peercy, J. M. Poate, D. C. Jacobson, A. G. Cullis, and N. G. Chew, Phys. Rev. Lett. **52**, 2360 (1984).
[3] M. O. Thompson, J. W. Mayer, A. G. Cullis, H. C. Webber, N. G. Chew, J. M. Poate, and D. C. Jacobson, Phys. Rev. Lett. **50**, 896 (1983).
[4] J. M. Poate and J. W. Mayer, eds., *Laser Annealing of Semiconductors* (Academic, New York, 1982).
[5] S. R. Stiffler, M. O. Thompson, and P. S. Peercy, Phys. Rev. Lett. **60**, 2519 (1988).
[6] W. Sinke and F. W. Saris, Phys. Rev . Lett. **53**, 2121 (1984).
[7] J. Narayan, S. J. Pennycook, D. Fathy, and O. W. Holland, J. Vac. Sci. Technol. A **2**, 1495 (1984).
[8] D. H. Lowndes, G. E. Jellison, S. J. Pennycook, S. P. Withrow, and D. N. Mashburn, Appl. Phys. Lett. **48**, 1389 (1986).
[9] J. J. P. Bruines, R. P. M. van Hal, H. M. J. Boots, A. Polman, and F. W. Saris, Appl. Phys. Lett. **49**, 1160 (1986).
[10] D. H. Lowndes, S. J. Pennycook, G. E. Jellison, S. P. Withrow, and D. N. Mashburn, J. Mater. Res. **2**, 648 (1987).
[11] K. Murakami, O. Eryu, K. Takita, and K. Masuda, Phys. Rev. Lett. **59**, 2203 (1987).
[12] P. S. Peercy, J. Y. Tsao, S. R. Stiffler, and M. O. Thompson, Appl. Phys. Lett. **52**, 203 (1988).
[13] J. Y. Tsao and P. S. Peercy, Phys. Rev. Lett. **58**, 2782 (1987).
[14] S. Roorda and W. C. Sinke, Appl. Surf. Sci. **36**, 188 (1989).
[15] D. H. Auston, C. M. Surko, T. N. C. Venkatesan, R. E. Slusher, and J. A. Golovchenko, Appl. Phys. Lett. **33**, 437 (1978).
[16] A complex refractive index of $4.05–0.045i$ was used, obtained from extrapolation of data by G. E. Jellison and H. H. Burke, J. Appl. Phys. **60**, 841 (1986) and M. O. Lampert, J. M. Koebel, and P. Siffert, J. Appl. Phys. **52**, 4975 (1981). The error in the velocity is determined by the estimated uncertainty in index (5%), the system timing inaccuracy (3%), and the standard deviation in the velocity data determined as a function of depth (5%).
[17] A. Polman, P. A. Stolk, D. J. W. Mous, W. C. Sinke, C. W. T. Bulle-Lieuwma, and D. E. W. Vandenhoudt (unpublished).
[18] P. A. Stolk, A. Polman, W. C. Sinke, C. W. T. Bulle-Lieuwma, and D. E. W. Vandenhoudt, Mater. Res. Soc. Proc. **147** (in press).
[19] A. G. Cullis, H. C. Webber, and N. Chew, Appl. Phys. Lett. **40**, 998 (1982).